"Environmental Engineering" 10th International Conference
Vilnius Gediminas Technical University
Lithuania, 27–28 April 2017
http://enviro.vgtu.lt

eISSN 2029-7092 / eISBN 978-609-476-044-0

Article ID: enviro.2017.037
DOI: https://doi.org/10.3846/enviro.2017.037

Triple Blending with Superfine Natural Zeolite and Condensed Silica Fume to Improve Performance of Cement Paste

P.L. Ng[1], J.J. Chen[2], A.K.H. Kwan[3]

[1]Faculty of Civil Engineeing, Vilnius Gediminas Technical University, Sauletekio Al.11, Vilnius LT-10223,Lithuania
[2]Department of Civil Engineering, Foshan University, 18 Jiangwan Road, Foshan, Guangdong Province, China
[3]Department of Civil Engineering, the University of Hong Kong, Pokfulam, Hong Kong, China
E-mails: [1]irdngpl@gmail.com (presenter); [2]chenjiajian@fosu.edu.cn (corresponding author); [3]khkwan@hku.hk

Abstract. Superfine natural zeolite (SNZ) is obtained by grinding natural zeolite to micro-fine size, whereas condensed silica fume (CSF) is by-product of ferrosilicon industry. Both SNZ and CSF are environmentally-friendly supplementary cementitious materials for mortar and concrete production. Owing to the high fineness and favourable grading of SNZ and CSF (the median particle sizes were 4 μm and 0.4 μm, respectively), the addition of SNZ and CSF could successively fill the voids between ordinary Portland cement (OPC) grains and increase the packing density of the binder, so as to reduce the volume of voids to be filled with water. Therefore, triple blending of OPC+SNZ+CSF can benefit the overall performance of cement paste by releasing more water for flowability improvement at the same water/binder (W/B) ratio, or adopting a lower W/B ratio for strength improvement at the same flowability requirement. This study evaluated the effects of adding SNZ and CSF on the packing density and water film thickness of binder. The experimental results proved that triple blending with SNZ and CSF could increase the packing density and improve the flowability and cohesiveness of cementitious paste.

Keywords: cohesiveness, condensed silica fume, flowability, packing density, superfine natural zeolite.

Conference topic: Environmental protection.

Introduction

As a naturally-occurring aluminosilicate mineral containing a high proportion (>60%) of silica (Ahmadi, Shekarchi 2010), natural zeolite can be grounded to micro-fine size to form superfine natural zeolite (SNZ) for use as a binder in mortar and concrete. The grinding of zeolite to a finer size than ordinary Portland cement (OPC) allows the zeolite particles to fill into the voids between cement grains and increase the packing density of the binder phase. In this regard, zeolite offers a remarkable advantage of having a relatively low hardness and thus requiring less energy input in the grinding process. In terms of the Moh's hardness scale, zeolite has a hardness of 2 to 3 (Sand, Mumpton 1976; Nagrockiene, Girskas 2016), whereas blast-furnace slag has a hardness of 6 to 7 or even higher than 7 (Xie *et al*. 2016). Therefore, the use of ground zeolite as a binder could lead to substantial savings in cost and energy.

Silica fume is by-product of ferrosilicon industry. It is derived from the production process of silicon metal and ferrosilicon alloys, and is mainly composed of silicon dioxide (about 95%) in an amorphous form. Silica fume is often densified to become condensed silica fume (CSF) for use in mortar and concrete (Malhotra *et al*. 1987; ACI Committee 234 2006). CSF can enhance the performance of mortar and concrete by way of both physical and chemical aspects. Having an extremely small particle size, CSF particles can fill into the voids between other powder particles and further increase the packing density of solids in the binder, as well as improve the interfacial transition zone and ameliorate the bleeding problem. The high SiO_2 content and large surface area of CSF render it a highly reactive pozzolana that reacts with lime from cement hydration to form additional gel (Kwan 2000).

While CSF has long been used in high-performance mortar and concrete production (Malhotra *et al*. 1987; ACI Committee 234 2006), the use of zeolite in concrete has attracted wide research interest only in relatively recent years. Karakurt and Topçu (2011) showed that the incorporation of ground zeolite could reduce the alkali-silica reaction and improve the sulphate resistance of concrete. Najimi *et al*. (2012) found that the addition of ground zeolite as partial cement replacement could lower the chloride ion penetration, water penetration and drying shrinkage of concrete. Ranjbar *et al*. (2013) successfully used ground zeolite to produce self-consolidating concrete with satisfactory flowability, cohesiveness and passing ability. Dousti *et al*. (2013) demonstrated that the addition of ground zeolite could lower the chloride permeability, though ground zeolite is less effective than silica fume. Markiv *et al*. (2016) reported that adding ground zeolite to partially replace cement would increase the superplasticizer demand, decrease the drying shrinkage, but would increase the water penetration and freeze-thaw resistances.

From the above, it is seen that both SNZ and CSF are environmentally-friendly supplementary cementitious materials for mortar and concrete production. Their usage as cement replacement in concrete would reduce the cement consumption and thus lower the carbon footprint for enhancing the sustainability of concrete construction. By proportioning SNZ and CSF with suitable particle size ranges, the combined usage of both SNZ and CSF could successively fill the voids between OPC grains and increase the packing density of the binder, so as to reduce the volume of voids to be filled with water. Therefore, triple blending of OPC+SNZ+CSF can benefit the overall performance of cementitious paste by releasing more water for flowability improvement at the same water/binder (W/B) ratio, or adopting a lower W/B ratio for strength improvement at the same flowability requirement. This study evaluated the effects of adding SNZ and CSF on the packing density and rheology of binder phase. A testing programme of 10 binder materials samples for packing density measurement and 60 cementitious paste samples containing different amounts of SNZ, CSF and water for flowability and cohesiveness tests was launched, as reported herein.

Testing programme

Three types of binder materials, namely OPC, SNZ and CSF, were used. The OPC was of grade 42.5N whereas the SNZ was of clinoptilolite type. The chemical compositions of the binder materials and their loss on ignition (L.O.I.) values are given in Table 1. The particle size distributions of OPC, SNZ and CSF were measured using a laser diffraction particle size analyzer and the results are plotted in Fig. 1. Based on these particle size distributions, the specific surface areas and the median particle size D_{50} (particle size of which 50% is smaller and 50% is larger) were determined. The physical properties of the binder materials including the solid densities measured in accordance with European Standard EN 196: part 6: 2010 (CEN 2010a), specific surface areas and median particle size are listed in Table 2.

Table 1. Chemical compositions (in %) of the binder materials

Chemical compositions	Ordinary Portland cement	Superfine natural zeolite	Condensed silica fume
Silicon dioxide (SiO_2)	22.9	62.9	95.5
Calcium oxide (CaO)	57.5	2.7	0.3
Aluminium oxide (Al_2O_3)	7.4	13.5	0.1
Iron(III) oxide (Fe_2O_3)	3.1	1.4	0.1
Magnesium oxide (MgO)	4.1	2.4	0.9
Loss on ignition (L.O.I.)	2.1	13.1	2.5
Water	–	≤ 1.5	≤ 0.5

Table 2. Physical properties of the binder materials

Physical properties	Ordinary Portland cement	Superfine natural zeolite	Condensed silica fume
Solid density (kg/m^3)	3127	2241	2212
Specific surface area ($\times 10^6$ m^2/m^3)	1.14	2.73	13.3
Specific surface area (m^2/kg)	368	1239	6045
Median particle size (μm)	9.34	3.55	0.38

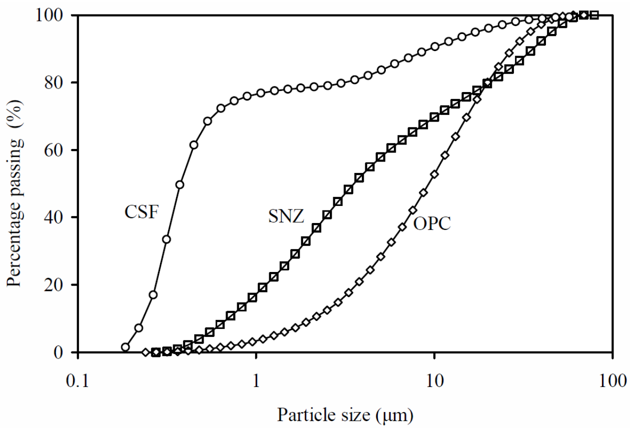

Fig. 1. Particle size distributions of the binder materials

The testing programme consisted of two parts. The first part was to measure the wet packing densities of the binder materials samples containing different amounts of SNZ and CSF for evaluating the effects of triple blending on packing density and water film thickness (WFT). The second part was to measure the flow spread, flow rate and cohesiveness of cementitious paste samples containing different amounts of SNZ and CSF at different W/B ratios for evaluating the effects of triple blending on rheological properties. The W/B ratio is expressed as the ratio of water content to binder materials content by mass. Each cementitious paste sample was assigned a mix number of (SNZ content)-(CSF content)-(W/B ratio). Both the SNZ and CSF contents are expressed as percentages by mass of the total binder materials. To avoid mixing up the effects of SNZ and/or CSF on rheology with the effects of superplasticizer, no superplasticizer was used in this study.

For both parts of the testing programme, the SNZ content was varied from 0 to 20% in increments of 5% while the CSF content was varied at 0 or 10%. In the first part, 10 blended binder materials samples were produced for packing density measurement. From the measured packing density of each sample, the corresponding voids ratio was calculated. These results were used to determine the WFT of the cementitious paste samples. In the second part, for each mix proportion of SNZ and CSF, the W/B ratio was varied from 0.45 to 0.70 in increments of 0.05. In total, 60 cementitious paste samples were produced for rheology tests. To ensure thorough mixing of the paste samples, the binder materials were added in several portions to and mixed with the water, rather than mixing all the binder materials and water in one go. This mixing procedure has been proven advantageous when the content of superfine size materials is high (Kwan, Wong 2008).

Test methods

Measurement of packing density

The wet packing test method was used to measure the packing density of each binder materials sample (Kwan, Wong 2008; Wong, Kwan 2008). To perform the test, 6 to 8 binder paste samples having the same mix proportions of binder materials but different water contents ranging from less than sufficient to more than sufficient to fill the voids between solid particles were produced. The respective bulk densities of the paste samples were measured to determine the corresponding solid concentrations (i.e. the solid volume to bulk volume ratio). In general, along with increasing the water content, the solid concentration first increased until reaching a maximum value and then decreased. The packing density of the binder materials is determined as the maximum solid concentration achieved by the binder paste samples.

From the measured packing density, the voids content (i.e. the ratio of the volume of voids to the bulk volume of the granular material) of each binder materials sample can be calculated as 1.0 minus the packing density. Then, the amount of excess water (i.e. water in excess of that needed for filling the voids between binder materials) in each paste sample was determined, and the WFT was evaluated as the excess water to solid surface area ratio:

$$\mathrm{WFT} = u_w'/A_S \tag{1}$$

The numerator is the excess water ratio u_w'. It carries the physical meaning of the ratio of the volume of excess water to the solid volume of all particles, and is given by

$$u_w' = u_w - u \tag{2}$$

where u_w is the water ratio (i.e. the ratio of volume of water to the solid volume of all particles) and u is the minimum voids ratio (i.e. the minimum ratio of volume of voids to the solid volume of the granular material). The denominator is the specific surface area A_S. It carries the physical meaning of the solid surface area per unit solid volume of all the particles, and is evaluated from the particle size distributions of the binder materials.

Measurement of flowability

The mini slump cone test was used to measure the flow spread, while the Marsh cone test was used to measure the flow rate (Aïtcin 1998). To perform the mini slump cone test, the slump cone was placed at the centre of a levelled steel plate, the cementitious paste was poured slowly into the slump cone until it was full, the slump cone was gently lifted and the flow spread was determined as the average diameter of the paste patty formed minus the base diameter of the slump cone. Any observation of bleeding was recorded during the test. To perform the Marsh cone test, the orifice of the Marsh cone was first closed, the cementitious paste was poured slowly into the Marsh cone until it was full, the orifice was opened to allow the paste to flow out, the flow time was recorded and finally the flow rate was determined as the volume of paste divided by the flow time.

Measurement of cohesiveness

The cohesiveness of the cementitious paste samples was measured using a modified version of the sieve segregation test stipulated in European Standard EN 12350: part 11: 2010 (CEN 2010b). This modified sieve segregation test for paste employed a 0.6 mm sieve instead of the 5.0 mm sieve in EN 12350: part 11: 2010. To perform the test, an approximately 0.1 litre cementitious paste sample was poured onto the sieve from a height of 300 mm and allowed to drip through the sieve. After two minutes, when the dripping had finished, the paste dripped through the sieve and collected by a base receiver was weighed and the sieve segregation index (SSI) was determined as the proportion of paste collected by the base receiver, expressed as a percentage by mass. A more cohesive paste would have a smaller proportion dripped through the sieve. On the contrary, a less cohesive paste would have a higher proportion dripped through the sieve. Hence, a low SSI indicates a high cohesiveness and a high segregation stability, and vice versa.

Test results

Packing density

The wet packing density results are listed in the second column of Table 3. With neither SNZ nor CSF added, the cement paste had a packing density of 0.543. With 10% SNZ added, the packing density was increased to 0.562; with 10% CSF added, the packing density was increased to 0.608; while with 10% SNZ and 10% CSF added, the packing density was further increased to 0.630. With 20% SNZ and 10% CSF added, the packing density was further increased to 0.645. For ease of visualisation, the variations of the packing density and voids ratio are plotted in Fig. 2. The results clearly show that the addition of SNZ and/or CSF can improve the packing density of cementitious materials. Relatively, CSF is more effective than SNZ because of its much finer size to fill into the voids between cement particles. Compare to double-blending, triple-blending the cementitious materials can further increase the packing density due to the successive filling of the voids between the larger particles.

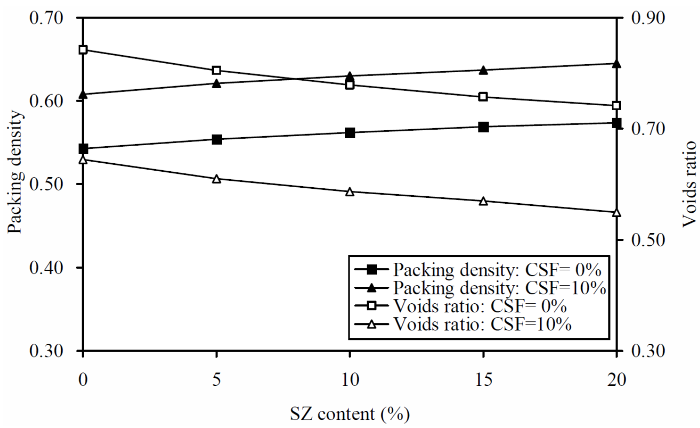

Fig. 2. Variations of packing density and voids ratio

Table 3. Test results of cementitious paste

Mix no.	Packing density	WFT (μm)	Flow spread (mm)	Flow rate (ml/s)	0.6 mm SSI (%)
0-0-0.45	0.543	0.486	166	32	9.4
0-0-0.50		0.622	227	72	15.6
0-0-0.55		0.758	236	108	18.6
0-0-0.60		0.894	296	121	27.1
0-0-0.65		1.030	312	138	44.6
0-0-0.70		1.166	344	153	70.6
5-0-0.45	0.554	0.450	128	21	7.5
5-0-0.50		0.571	197	63	18.7
5-0-0.55		0.693	207	83	14.6
5-0-0.60		0.815	246	113	27.6
5-0-0.65		0.936	296	133	48.4
5-0-0.70		1.058	321	141	51.8
10-0-0.45	0.562	0.414	100	13	3.2
10-0-0.50		0.524	165	38	9.1
10-0-0.55		0.634	217	85	14.6
10-0-0.60		0.744	230	109	21.2
10-0-0.65		0.854	285	117	36.3
10-0-0.70		0.964	291	129	45.5

End of Table 3

Mix no.	Packing density	WFT (μm)	Flow spread (mm)	Flow rate (ml/s)	0.6 mm SSI (%)
15-0-0.45	0.569	0.383	103	13	0.3
15-0-0.50		0.483	156	36	4.6
15-0-0.55		0.583	199	57	7.5
15-0-0.60		0.684	199	94	16.1
15-0-0.65		0.784	267	110	18.3
15-0-0.70		0.884	288	120	35.4
20-0-0.45	0.574	0.352	97	14	0.7
20-0-0.50		0.445	131	30	6.3
20-0-0.55		0.537	181	44	6.7
20-0-0.60		0.629	201	78	5.9
20-0-0.65		0.721	226	107	22.2
20-0-0.70		0.814	278	114	28.8
0-10-0.45	0.608	0.250	2	0	0.0
0-10-0.50		0.303	27	0	0.0
0-10-0.55		0.357	67	2	0.0
0-10-0.60		0.410	95	10	3.8
0-10-0.65		0.463	130	20	8.3
0-10-0.70		0.517	175	35	14.9
5-10-0.45	0.621	0.246	1	0	0.0
5-10-0.50		0.297	8	0	0.0
5-10-0.55		0.348	49	4	0.0
5-10-0.60		0.399	89	9	3.5
5-10-0.65		0.451	118	22	6.2
5-10-0.70		0.502	137	29	11.7
10-10-0.45	0.630	0.240	1	0	0.0
10-10-0.50		0.289	16	0	0.0
10-10-0.55		0.337	29	0	0.0
10-10-0.60		0.386	74	8	0.0
10-10-0.65		0.435	99	20	3.8
10-10-0.70		0.484	125	36	7.9
15-10-0.45	0.637	0.232	0	0	0.0
15-10-0.50		0.279	12	0	0.0
15-10-0.55		0.326	26	0	0.0
15-10-0.60		0.373	70	11	0.0
15-10-0.65		0.420	86	23	0.0
15-10-0.70		0.467	111	40	3.1
20-10-0.45	0.645	0.226	0	0	0.0
20-10-0.50		0.271	14	0	0.0
20-10-0.55		0.316	20	0	0.0
20-10-0.60		0.361	57	12	0.0
20-10-0.65		0.406	76	27	0.0
20-10-0.70		0.451	95	51	1.9

Water film thickness

The WFT of the paste samples are tabulated in the third column of Table 3 and plotted against the W/B ratio in Fig. 3. In theory, the reduction in voids ratio due to the addition of SNZ and/or CSF would decrease the amount of water needed to fill the voids and thus increase the amount of excess water available for forming water films coating the solid particles. However, the WFT is dependent also on the total surface area of the particles and the water content (Kwan, Wong 2008; Ng *et al*. 2016). From the WFT curves, it can be seen that despite the resulting increase in packing density and decrease in voids ratio, the addition of SNZ and/or CSF would still decrease the WFT because of the proportionally larger increase in specific surface area.

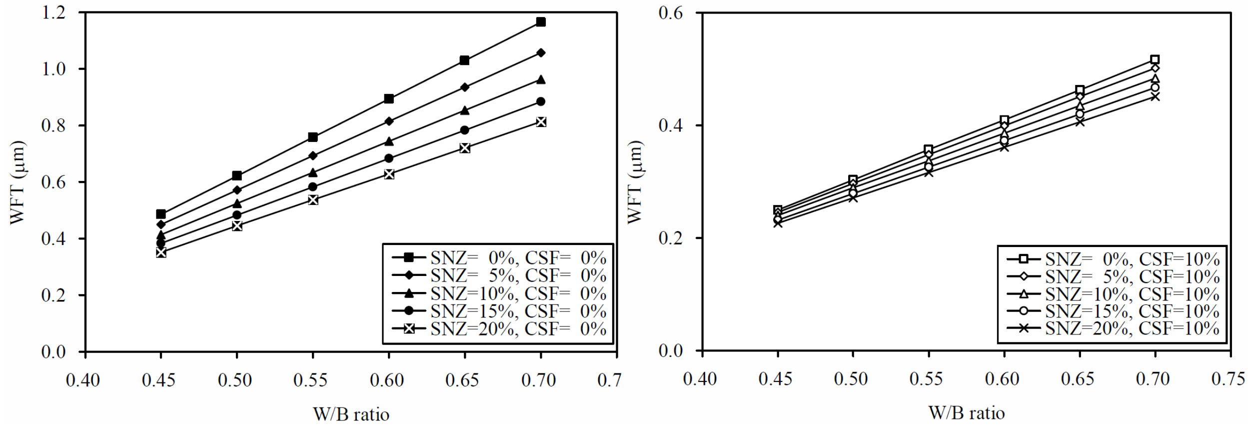

(a) CSF = 0%

(b) CSF = 10%

Fig. 3. Variations of water film thickness

Flow spread

The flow spread results are tabulated in the fourth column of Table 3 and plotted graphically in Fig. 4. It is evident from the flow spread curves that regardless of SNZ content, addition of CSF as cement replacement would dramatically decrease the flow spread at the same W/B ratio. On the other hand, with the absence or presence of CSF, the addition of SNZ would gradually decrease the flow spread at the same W/B ratio. For instance, at a W/B ratio of 0.60, the addition of 20% SNZ decreased the flow spread from 296 to 201 mm when no CSF was added, while the addition of 20% SNZ decreased the flow spread from 95 to 57 mm when 10% CSF was added. The effects of SNZ and CSF may be attributed to the increases in packing density and surface area of binder materials.

During the flow spread test, bleeding was observed for the mixes with W/B ratio of 0.70 and with 0% or 5% SNZ and no CSF added. The data points for the mixes that exhibited bleeding are circled in Fig. 3. It is noted that the addition of 10% or more SNZ or 10% CSF could prevent the occurrence of bleeding at a W/B ratio of as high as 0.70. The effectiveness of SNZ or CSF in alleviating bleeding can be explained by the improvement in cohesiveness due to the addition of superfine or ultrafine particles.

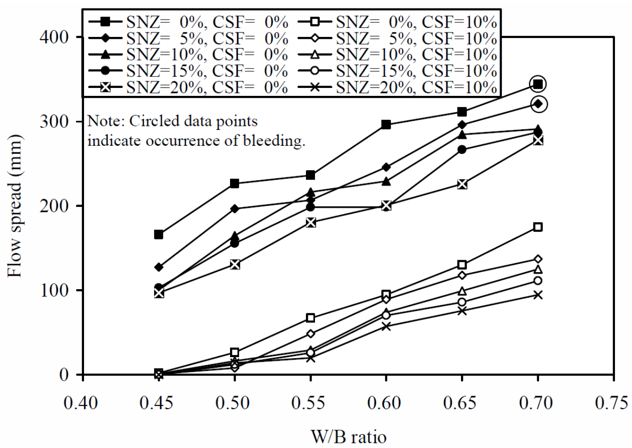

Fig. 4. Variation of flow spread

Flow rate

The flow rate results are tabulated in the fifth column of Table 3 and plotted in Fig. 5. The flow rate curves show that regardless of SNZ content, addition of CSF as cement replacement would dramatically decrease the flow rate at the same W/B ratio (similar to the effect on flow spread). On the other hand, the results indicated that when no CSF was added, the addition of SNZ as cement replacement tended to decrease the flow rate of the cementitious paste at the same W/B ratio. However, when 10% CSF was added, the effect of addition of SNZ on flow rate is rather complicated: at a W/B ratio equal to or below 0.55, the addition of SNZ would generally decrease the flow rate; at a W/B ratio equal to or above 0.60, the addition of SNZ would increase or decrease the flow rate. The effects of SNZ and CSF may be attributed to the combined effects of decrease in voids ratio and increase in surface area of binder materials, as well as increase in cohesiveness and slurry effect of the cementitious paste.

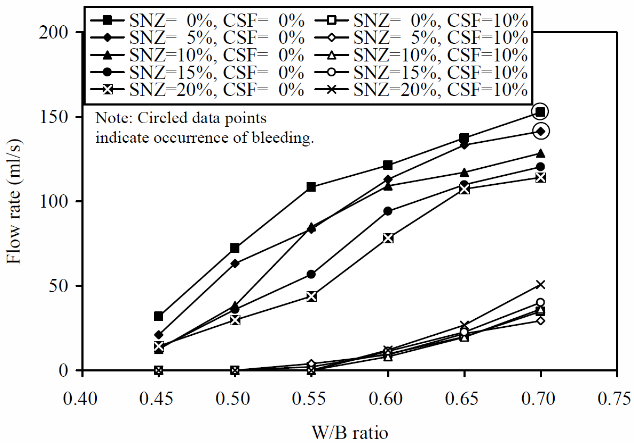

Fig. 5. Variation of flow rate

Cohesiveness

The 0.6 mm SSI results are listed in the sixth column of Table 3 and plotted against the W/B ratio at different SNZ and CSF contents in Fig. 6. It can be seen that at a constant W/B ratio, the addition of SNZ and/or CSF as cement replacement would decrease the SSI and hence increase the cohesiveness. Relatively, the effect of CSF is more significant than that of SNZ. Such increase in cohesiveness may be attributed to the bridging effect of SNZ and CSF particles, which would fill into the gaps between cement grains, and the reduction in WFT as will be presented later.

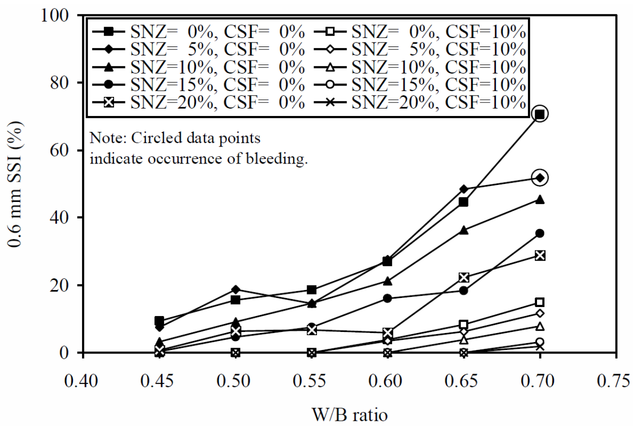

Fig. 6. Variation of 0.6 mm SSI

Discussions

Role of water film thickness in rheology

To study the role of WFT in the rheology, the flow spread results are plotted against the WFT for different SNZ and CSF contents in Fig. 7. It can be observed that all the data points fall within a narrow band. This reveals that the WFT has great effect on the flow spread. As reflected by the general trend of variation of the data points, the flow spread increased with the WFT at a gradually diminishing rate. Regression analysis has been carried out to correlate the flow spread with the WFT. The best-fit equation and curve so obtained are presented alongside the data points in Fig. 7. A very high R^2 value of 0.976 has been achieved, indicating that the flow spread is governed solely by the WFT and that the addition of SNZ and/or CSF exerts its influence on the flow spread mainly by changing the WFT.

Apart from the flow spread, the flow rate results are plotted against the WFT for different SNZ and CSF contents in Fig. 8. As reflected by the general trend of variation of the data points, when the WFT was smaller than 0.36 µm, the flow rate remained at approximately zero; when the WFT was larger than 0.36 μm, the flow rate increased with the WFT at a gradually diminishing rate. The flow rate has been correlated with the WFT by regression analysis. The best-fit equation and curve so obtained are presented alongside the data points in Fig. 8. The correlation yielded a very high R^2 value of 0.968, indicating that the flow rate is governed solely by the WFT and that the addition of SNZ and/or CSF exerts its influence on the flow rate mainly by changing the WFT.

To illustrate the effects of SNZ and/or CSF content and WFT on cohesiveness, the 0.6 mm SSI results are plotted against the WFT for different SNZ and CSF contents in Fig. 9.

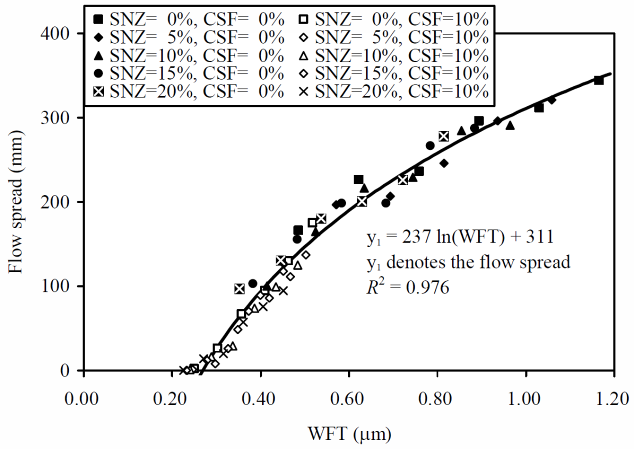

Fig. 7. Flow spread versus water film thickness

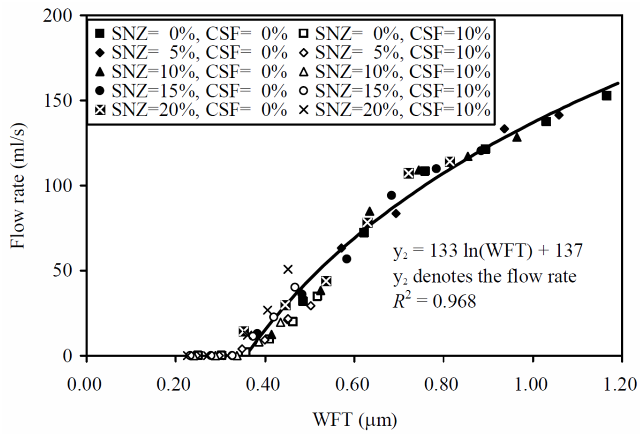

Fig. 8. Flow rate versus water film thickness

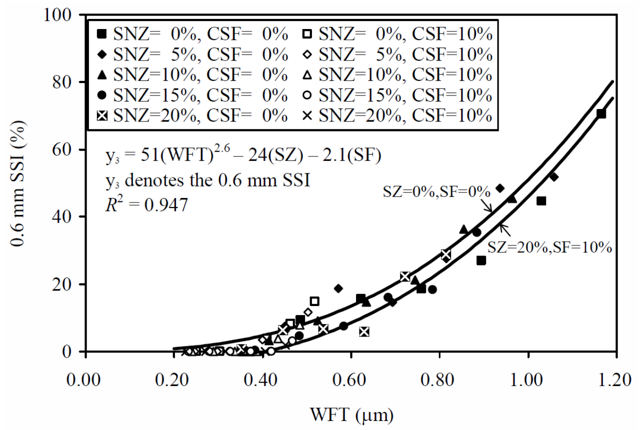

Fig. 9. 0.6 mm SSI versus water film thickness

By means of multi-variable regression analysis, the 0.6 mm SSI is correlated to the WFT and the SNZ and CSF contents. The best-fit equation and the curves so obtained are presented alongside the data points in Fig. 9. It can be seen that the 0.6 mm SSI-WFT curves diverged in such a way that at the same WFT, a cementitious paste having a higher SNZ and/or CSF content would have a lower 0.6 mm SSI, i.e., higher cohesiveness. This may be attributed to the effects of SNZ and CSF to increase the surface area and thus increase the electrostatic attractive forces between solid particles. The correlation yielded a R^2 value of 0.947, indicating that the cohesiveness is governed mainly by the WFT and partially by the SNZ and CSF contents.

Concurrent cohesiveness-flow rate performance

The effects of SNZ and CSF addition on the concurrent cohesiveness-flow rate performance of cementitious paste are elucidated by plotting the 0.6 mm SSI against the flow rate in Fig. 10. Each performance curve in the figure is a plot of the SSI and flow rate that could be concurrently achieved at a fixed SNZ and/or CSF content. It is evident from Fig. 10 that the addition of SNZ with absence or presence of CSF would shift the curves downwards and to the right. This indicates that SNZ was capable of increasing the cohesiveness at the same flow rate, increasing the flow rate at the same cohesiveness, or increasing both the cohesiveness and flow rate simultaneously. Furthermore, the addition of SNZ would reduce the cement consumption and hence reduce the carbon footprint and the cost of concrete production. Such great benefits of SNZ are paramount to the production of green concrete with stringent demand on flow rate and cohesiveness, such as self-consolidating concrete, tremie concrete and pumped concrete.

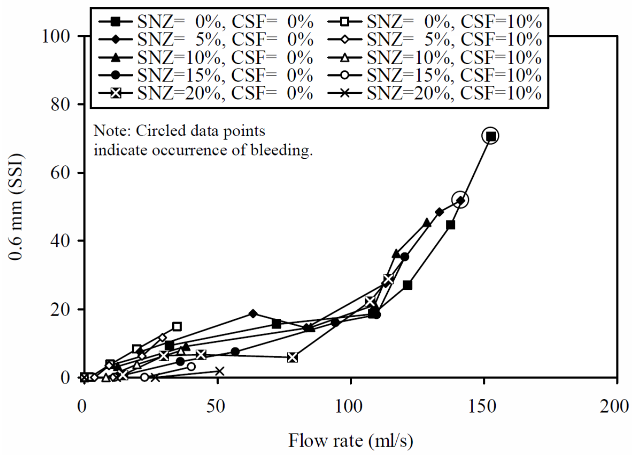

Fig. 10. Concurrent cohesiveness and flow rate performance

Conclusions

To evaluate the effects of combined addition of SNZ and CSF on the rheological performance of cementitious paste, an experimental programme comprising 10 mixes of blended binder materials for packing density measurement, and 60 cementitious paste samples with W/B ratios between 0.45 and 0.70 for flowability and cohesiveness tests, was implemented. The WFT of the paste samples was evaluated from the known W/B ratios and measured packing densities, and its role in the rheological performance has been studied. The following conclusions may be drawn: (1) Double blending of OPC+SNZ or OPC+CSF, and triple blending of OPC+SNZ+CSF could increase the packing density. Relatively, the finer CSF was more effective in improving packing density. However, the addition of SNZ and/or CSF at a W/B ratio between 0.45 and 0.70 would decrease the WFT. (2) Blending with SNZ and/or CSF would decrease the flow spread and flow rate mainly through its consequential change to the WFT. (3) Blending with SNZ and/or CSF would significantly improve the cohesiveness and stability against segregation. (4) The addition of SNZ was able to improve the concurrent cohesiveness-flow rate performance. Moreover, the use of SNZ can reduce the cement consumption and hence the carbon footprint and the cost of concrete production.

Funding

The work presented in this paper was supported by funding from Natural Science Foundation of Guangdong Province of China (Project No. 2014A030310273), Science and Technology Project of Foshan City of China (Project No. 2016AB000031), and Marie Skłodowska-Curie Actions of the European Commission (Project No. 751461).

Disclosure statement

The authors confirm that they do not have any competing financial, professional, or personal interests from other parties.

References

ACI Committee 234. 2006. *ACI 234R-06: Guide for the Use of Silica Fume in Concrete*. Detroit, USA: American Concrete Institute.

Ahmadi, B.; Shekarchi, M. 2010. Use of natural zeolite as a supplementary cementitious material, *Cement and Concrete Composites* 32(2): 134–141. https://doi.org/10.1016/j.cemconcomp.2009.10.006

Aïtcin, P.-C. 1998. *High-performance concrete*. E&FN Spon, London, UK and New York, USA. 591 p. https://doi.org/10.4324/9780203475034

Comité Européen de Normalisation (CEN). 2010a. *EN 196-6: 2010: Methods of testing cement – part 6: Determination of fineness*. Brussels, Belgium: Comité Européen de Normalisation.

Comité Européen de Normalisation (CEN). 2010b. *EN 12350-11: 2010: Testing of fresh concrete – part 11: Self-compacting concrete - seieve segregation test*. Brussels, Belgium: Comité Européen de Normalisation.

Dousti, A.; Rashetnia, R.; Ahmadi, B.; Shekarchi, M. 2013. Influence of exposure temperature on chloride diffusion in concretes incorporating silica fume or natural zeolite, *Construction and Building Materials* 49: 393–399. https://doi.org/10.1016/j.conbuildmat.2013.08.086

Karakurt, C.; Topçu, İ. B. 2011. Effect of blended cements produced with natural zeolite and industrial by-products on alkali-silica reaction and sulfate resistance of concrete, *Construction and Building Materials* 25(4): 1789–1795. https://doi.org/10.1016/j.conbuildmat.2010.11.087

Kwan, A. K. H. 2000. Use of condensed silica fume for making high-strength, self-consolidating concrete, *Canadian Journal of Civil Engineering* 27(4): 620–627. https://doi.org/10.1139/l99-091

Kwan, A. K. H.; Wong, H. H. C. 2008. Packing density of cementitious materials: part 2 – packing and flow of OPC + PFA + CSF, *Materials and Structures* 41(4): 773–784. https://doi.org/10.1617/s11527-007-9281-6

Malhotra, V. M.; Ramachandran, V. S.; Feldman, R. F.; Aictin, P.-C. 1987. *Condensed silica fume in concrete*. CRC Press, USA. 221 p.

Markiv, T.; Sobol, K.; Franus, M.; Franus, W. 2016. Mechanical and durability properties of concretes incorporating natural zeolite, *Archives of Civil and Mechanical Engineering* 16(4): 554–562. https://doi.org/10.1016/j.acme.2016.03.013

Najimi, M.; Sobhani, J.; Ahmadi, B.; Shekarchi, M. 2012. An experimental study on durability properties of concrete containing zeolite as a highly reactive natural pozzolan, *Construction and Building Materials* 35: 1023–1033. https://doi.org/10.1016/j.conbuildmat.2012.04.038

Nagrockiene, D.; Girskas, G. 2016. Research into the properties of concrete modified with natural zeolite addition, *Construction and Building Materials* 113: 964–969. https://doi.org/10.1016/j.conbuildmat.2016.03.133

Ng, P. L.; Chen, J. J.; Kwan, A. K. H. 2016. Improving particle size distribution in cement paste by blending with superfine cement, *Journal of Sustainable Architecture and Civil Engineering* 16(3): 108–120. https://doi.org/10.5755/j01.sace.16.3.16273

Ranjbar, M. M.; Madandoust, R.; Mousavi, S. Y.; Yosefi, S. 2013. Effects of natural zeolite on the fresh and hardened properties of self-compacted concrete, *Construction and Building Materials* 47: 806–813. https://doi.org/10.1016/j.conbuildmat.2013.05.097

Sand, L. B.; Mumpton, F. A. 1976. Natural zeolites: occurrence, properties, and use, in *Proceedings of Zeolite Conference*, June 1976, Tucson, Arizona, USA. New York: Pergamon Press.

Wong, H. H. C.; Kwan, A. K. H. 2008. Packing density of cementitious materials: part 1 – measurement using a wet packing method, *Materials and Structures* 41(4): 689–701. https://doi.org/10.1617/s11527-007-9274-5

Xie, J.; Wu, S.; Zhang, L.; Xiao, Y.; Ding, W. 2016. Evaluation the deleterious potential and heating characteristics of basic oxygen furnace slag based on laboratory and in-place investigation during large-scale reutilization, *Journal of Cleaner Production* 133: 78–87. https://doi.org/10.1016/j.jclepro.2016.05.106